External control of the scattering properties of a single optical nanoantenna

C. Huang,[1] A. Bouhelier,[1,a)] J. Berthelot,[1] G. Colas des-Francs,[1] E. Finot,[1] J.-C. Weeber,[1] A. Dereux,[1] S. Kostcheev,[2] A.-L. Baudrion,[2] J. Plain,[2] R. Bachelot,[2] P. Royer,[2] and G. P. Wiederrecht[3]

[1]*Laboratoire Interdisciplinaire Carnot de Bourgogne, CNRS UMR-5209, Université de Bourgogne, Dijon, Bourgogne 21000, France*

[2]*Laboratoire de Nanotechnologie et d'Instrumentation Optique, Institut Charles Delauney, Université Technologique de Troyes, Troyes 10010, France*

[3]*Center for Nanoscale Materials, Argonne National Laboratory, Argonne, Illinois 60439, USA*

(Received 24 November 2009; accepted 17 March 2010; published online 7 April 2010)

We present a mechanism to control the scattering properties of individual optical nanoantennas by applying an external electric field. We find that by electrically tuning an anisotropic load medium the scattered intensity becomes voltage-dependent. We also demonstrate that the scattering diagram of the antenna can be externally adjusted. This on-demand command opens up the possibility to tune an antenna without changing its geometrical parameters. © *2010 American Institute of Physics*. [doi:10.1063/1.3385155]

Optical antennas are devices utilized to interface far-field radiation to localized regions and vice-versa.[1,2] They are the basis for diverse applications ranging from highly sensitive biosensors,[3] to nanoscale photodetectors.[4] The capability of antennas to concentrate and redirect light is mainly inferred from design parameters and mutual interactions between antenna's constituents.[5–9] Another set of parameters that have been recently introduced to tailor the optical response of antennas are the impedance and the load of the device.[10–12]

In this paper, we demonstrate an external control over the elastic scattering properties of single dimer antennas constituted of two interacting gold nanoparticles. This is achieved by electrically modifying an anisotropic load medium surrounding the antennas, i.e., a nematic liquid crystals (LC). The orientation of the LC director, hence the anisotropy, can be adjusted by applying an electric potential. Previous work on gold nanoparticles demonstrated a modification of the spectral position of surface plasmon resonances as a consequence of the voltage sensitive-anisotropy.[12–16] To the difference with these studies, we report here on the modification of the radiation scattered by the antenna (intensity and scattering diagram) at a given operating wavelength. Gold antennas were prepared on a bare glass substrate by standard e-beam lithography and lift-off techniques. The dimer antennas consisted of two identical nanodisks (70 nm in diameter and 40 nm thick) precisely placed between two planar electrodes separated by 3.5 μm as shown in the images of Figs. 1(a) and 1(b). The feedgap between the disks was systematically varied from contact to about 100 nm. The orientation of dimers alternates from an axis parallel to the electrodes (x-direction) to an axis perpendicular (y-direction). Finally, each dimers are separated by 3 μm to avoid short-range coupling. A single isolated particle was also fabricated and served as reference antenna. The antennas and electrodes were immersed in the LC (E7© from Merck with a positive birefringence of $\Delta n = n_e - n_o = 0.2$) without introducing any pre-alignment layer. Transmission images taken under cross-polarizers indicated an homeotropic orientation of the LC director.[12] The in-plane switching of the LC director is controlled with an electric field U_{bias} varying up to 2.9 V/μm with a 1 KHz oscillating square waveform.

The scattering properties of the optical antennas were characterized by diascopic confocal-type microscope operating at $\lambda_{\text{laser}} = 633$ nm with an incident numerical aperture $\text{N.A.}_{\text{inc}} = 0.65$. A circular beam stop with a $\text{N.A.}_{\text{BS}} = 0.85$ placed at the Fourier plane of the microscope serves to reject the direct illumination wave-vectors ($\text{N.A.}_{\text{BS}} > \text{N.A.}_{\text{inc}}$).[17] Only wave-vectors scattered by the optical antennas and comprised between N.A._{BS} and the $\text{N.A.}_{\text{max}} = 1.45$ of the collection objective were detected [see Fig. 1(f)]. Optical antennas were scanned through the foci in order to reconstruct a diffraction-limited image of the scattered intensity $I_{\text{scat}}(x,y)$. To obtain the wave-vector spectrum, i.e., the emission diagram of the scattered light, a charge coupled device (CCD) detector placed in a conjugated Fourier plane of the microscope recorded the angular distribution of the intensity radiated in the substrate.[9,18] In order to simplify our research, we aimed at two polarizations states seen by the antenna corresponding to the x or y axis of the dimer, i.e., corrected for the

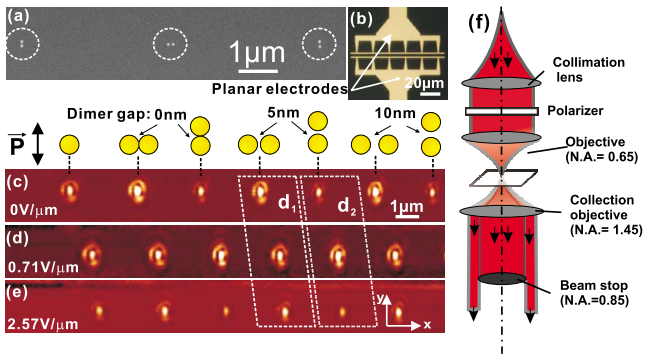

FIG. 1. (Color online) (a) Scanning electron micrograph of three dimer antennas (dashed circles) fabricated by electron beam lithography. The dimers were placed between two macroscopic planar electrodes as shown in the large scale optical image (b). (c)–(e) Confocal scan images of series of antennas obtained with a linear polarization (arrow) and for three values of U_{bias}. The bright spots correspond to the intensity scattered by individual dimers. (f) Schematics of the setup consisting on a low-NA diascopic illumination and a high-NA detection. A beam stop rejects the illumination wavevectors retaining only the large wavevectors scattered by the antennas.

a)Electronic mail: alexandre.bouhelier@u-bourgogne.fr.

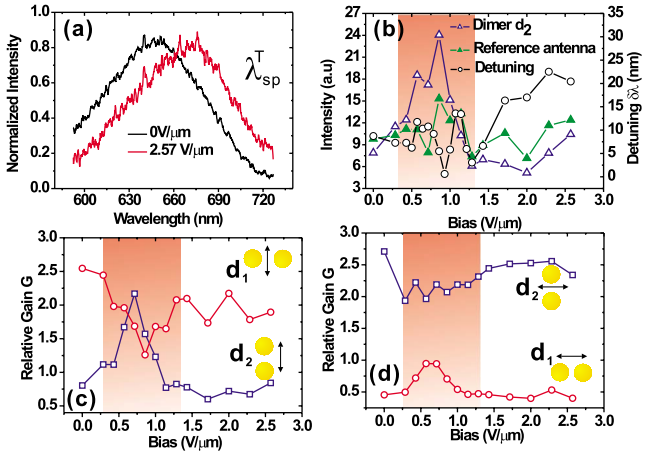

FIG. 2. (Color online) (a) Dark field spectra of the λ_{sp}^{T} of d_2 for two biases showing the plasmon shift. (b) Intensity and detuning as a function of U_{bias} for the reference and the dimer labeled d_2 and for a y-polarization. The intensity of d_2 is maximal when $|\Delta\lambda|$ is the smallest. The voltages comprised within the boxed red region corresponds to the Fréedericksz's transition of the LCs. (c) and (d) d_1 and d_2 relative gain G as a function of U_{bias} and for two polarizations. The active bias region is situated within the Fréedericksz's transition.

bias-dependent polarization change through the cell. Figures 1(c)–1(e) show $I_{\text{scat}}(x,y)$ for three U_{bias} applied to the electrodes. The polarization at the antenna was adjusted collinear to the field lines (y-direction). The first bright spot on the left-hand-side is the scattered signal issued from the reference antenna. At a null bias, the x-oriented dimers show an increased of I_{scat} with respect to both the reference particle and the y-oriented dimers. This increase does not significantly depend on the feedgap range considered here. Two phenomena play a role in the modification of I_{scat}. First, because the antenna are immersed in an index-varying medium, their ability to scatter radiation in the substrate is altered. Second, the variation in I_{scat} can be also understood in terms of a detuning factor $|\Delta\lambda|=|\lambda_{\text{laser}}-\lambda_{sp}|$ encoding the difference between the excitation wavelength λ_{laser} and the position of the dimers' longitudinal and transverse surface plasmon resonances $\lambda_{sp}^{L,T}$.[9] These resonances depend on the local refractive index, and for liquid crystals, on the applied voltage. This is illustrated in Fig. 2(a) for λ_{sp}^{T} of the dimer labeled d_2 in the boxed area of Fig. 1(c) undergoing a redshift for this polarization[12] already observed by Müller *et al.*[13] and discussed in terms of an increased molecular density. At null bias, I_{scat} is larger for the x-oriented dimers because the laser wavelength (633nm) is closer to the transverse resonances ($\sim$645 nm) than the redshifted longitudinal plasmon. For increasing U_{bias} [Figs. 1(d) and 1(e)], the intensities scattered by the dimer antennas are significantly modified. Figure 2(b) shows the nonmonotonous evolution of $I_{\text{scat}}^{d_2}$ for the dimer d_2 and for the reference antenna $I_{\text{scat}}^{\text{ref}}$ as a function of U_{bias}. The intensity scattered off the reference antenna has a weak dependence on U_{bias} with an average amplitude of 10 ± 2 (arbitrary unit). The shaded area in Fig. 2(b) delimiting $0.5\ \text{V}/\mu\text{m}<U_{\text{bias}}<1.25\ \text{V}/\mu\text{m}$ is the electric field range where $I_{\text{scat}}^{d_2}$ undergoes the most dramatic changes and corresponds to the onset of Fréedericksz's transition. This voltage threshold results from the competing torque imposed by the natural anchoring of the LC molecules and the torque caused by the external electric field.[12,19] This transition range was systematically observed for all the antennas. Furthermore, the scattered intensities showed very little hysteresis upon voltage sweep insuring thus reproducible and controlled measurements (data not shown).

Figure 2(b) also shows the detuning factor $|\Delta\lambda|$ where λ_{sp}^{L} was extracted from dark-field spectroscopy.[12] Here too, the largest detuning is obtained for field values comprised within the Fréedericksz's transitions. The exact orientation of the LC molecules in the vicinity of the antenna are difficult to determined solely from spectroscopic data. However, for this range of U_{bias} and polarization alignment, the surface plasmon resonance has redshifted by 25 nm from its position at null bias due to a locally higher refractive index. There is an opposite trend between the intensity scattered by d_2 and $|\Delta\lambda|$ demonstrating that I_{scat} is maximum when $|\Delta\lambda|\to0$. We therefore argue that detuning is probably more effective in modifying I_{scat} than the redirection of scattered power out of the detection angles.

In antenna theory, the ability of an antenna to increase scattered intensity in the direction of the peak radiation is usually normalized to a reference dipolar radiator.[9,20] We applied this formalism by normalizing the scattered intensities to that of the reference single-particle antenna. Our reference antenna being much smaller than the wavelength, its scattering properties can be considered dipolelike.[9] Figures 2(c) and 2(d) show the U_{bias}-dependency of the relative antenna gain $G=I_{\text{scat}}^{\text{dimer}}/I_{\text{scat}}^{\text{ref}}$ for two selected dimers d_1 and d_2 [Fig. 1(c)] and for two polarizations. For both cases, G is significantly altered by the onset of Fréedericksz's transitions. Outside of this range, the intensity does not dramatically change from G measured at a null bias. For a polarization oriented along the field lines [Fig. 2(c)], G is threefold increased for d_2 at $U_{\text{bias}}=0.75\ \text{V}/\mu\text{m}$. According to the trend outlined by Fig. 2(b), the orientation of the LC molecules is shifting the longitudinal plasmon resonance λ_{sp}^{L} closer to λ_{laser}. This is confirmed by the evolution of d_2 for x-polarization [Fig. 2(d)], probing the transverse resonance λ_{sp}^{T}. Because $\lambda_{sp}^{T}<\lambda_{sp}^{L}$, d_2 displays a minimum G around the same value of U_{bias}. The evolution of G for d_1 shows the same qualitative behavior with a drop of half of its magnitude at $U_{\text{bias}}=0.85\ \text{V}/\mu\text{m}$ for a y-polarization. The difference of G between d_1 and d_2 excited along a principal axis stems from their relative orientations with respect to the field lines which control the molecular orientation and refractive index hence $|\Delta\lambda|$ and G.

To complete our analysis, we measured the scattering diagram of the antennas by detecting the angular distribution of the intensity in a conjugated Fourier plane of the microscope. Prior to detection, the scattered intensity was spatially filtered by a 30 μm pinhole to remove a strong scattering contribution from the electrodes. Figures 3(a)–3(d) show a set of diagrams representing the angular distribution of the intensity scattered by the reference antenna. In this measurement, the field-dependence of the polarization orientation was not compensated and was adjusted to be along the y-direction at a null bias. Since our cell contained mostly a homeotropic alignment, the polarization at the entrance of the cell is oriented along n_o. The dipolar nature of the reference antenna under this polarization is recognized as a two-lobe pattern concentrating the scattered intensity [Fig. 3(a)]. When U_{bias} increases, the LC director gradually aligns with field lines in a planar arrangement imposing thus a rotation of the polarization between the electrodes. In our case, increasing U_{bias} above the Fréedericksz's transitions lead to a

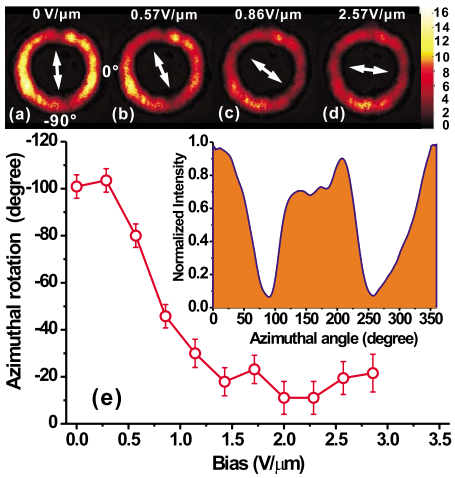

FIG. 3. (Color online) (a)–(d) False color CCD images of the angular distribution of the scattered intensity by the reference antenna as a function of applied electric field U_{bias} for a fixed incidence polarization. The orientation of the lobes is rotating with the bias. (e) Azimuthal orientation of the minima of the scattering diagrams as a function U_{bias} demonstrating the angular control of the scattering diagram. Inset: Averaged angular intensity distribution of the annular pattern in (a). Two minima are visible indicative of a lobe pattern.

close to 90° shift. The consequence of that shift is the rotation of the two-lobe pattern as a function of U_{bias} observed in Figs. 3(a)–3(d) and reported in Fig. 3(e) displaying the azimuthal position of the minimum of intensity [arrow in Fig. 3(a)] as a function of U_{bias}. The position of the minimum was extracted by a radial averaging of the azimuthal intensity profile as shown in the inset of Fig. 3(e). The reorientation of the LC molecules provides a mean to electrically control *in situ* the radiation diagram of a single optical antenna. Note that the rotation occurs in the Fréedericksz's region and the diagram of Fig. 3(h) does not significantly evolve for U_{bias} comprised between 1.42 V/μm and 2.57 V/μm. We attribute this behavior to the complex polarization state around the Fréedericksz's transient.[21] We have also recorded the scattering diagrams obtained for dimer-antenna d_2 as a function of U_{bias} for fixed x-polarization seen by the antenna. When the polarization is bias-compensated, the scattered diagrams do not drastically change their overall angular response (data not shown). The integrated intensity follows the evolution of $I_{\text{scat}}^{\text{ref}}$ measured in Fig. 2(d).

In summary, we have demonstrated that the radiation scattered by an individual optical antenna can be controlled with an external stimulus. This control is achieved by modifying the load medium of the antenna. We further show that the scattering diagrams can be electrically controlled by changing the polarization state around LC Fréedericksz's transitions. We believe the external command of the scattering characteristics can help to control an optical exchange without modifying the geometrical parameters of an antenna.

The authors thank the A.N.R. under grants Antares (PNANO 07-51), Photohybrid (BLANC 07-2-188654). Use of the Center for Nanoscale Materials was supported the U. S. Department of Energy, Office of Science, Office of Basic Energy Sciences, under Contract No. DE-AC02-06CH11357.

[1] J. N. Farahani, D. W. Pohl, H.-J. Eisler, and B. Hecht, Phys. Rev. Lett. **95**, 017402 (2005).
[2] P. Bharadwaj, B. Deutsch, and L. Novotny, Adv. Opt. Photon **1**, 438 (2009).
[3] S. S. Aćimović, M. P. Kreuzer, M. U. González, and R. Quidant, ACS Nano **3**, 1231 (2009).
[4] L. Tang, S. E. Kocabas, S. Latif, A. K. Okyay, D.-S. Ly-Gagnon, K. C. Saraswat, and D. A. B. Miller, Nat. Photonics **2**, 226 (2008).
[5] K. Li, M. I. Stockman, and D. J. Bergman, Phys. Rev. Lett. **91**, 227402 (2003).
[6] H. X. Xu and M. Käll, Phys. Rev. Lett. **89**, 246802 (2002).
[7] H. F. Hofmann, T. Kosako, and Y. Kadoya, New J. Phys. **9**, 217 (2007).
[8] T. H. Taminiau, F. D. Stefani, and N. F. van Hulst, Opt. Express **16**, 10858 (2008).
[9] C. Huang, A. Bouhelier, G. Colas des Francs, A. Bruyant, A. Guenot, E. Finot, J.-C. Weeber, and A. Dereux, Phys. Rev. B **78**, 155407 (2008).
[10] A. Alù and N. Engheta, Phys. Rev. Lett. **101**, 043901 (2008).
[11] M. Schnell, A. Garcia-Etxarri, A. J. Huber, K. Crozier, J. Aizpurua, and R. Hillenbrand, Nat. Photonics **3**, 287 (2009).
[12] J. Berthelot, A. Bouhelier, C. Huang, J. Margueritat, G. Colas-des-Francs, E. Finot, J. C. Weeber, A. Dereux, S. Kostcheev, H. I. Ahrach, A. L. Baudrion, J. Plain, R. Bachelot, P. Royer, and G. P. Wiederrecht, Nano Lett. **9**, 3914 (2009).
[13] J. Müller, C. Sonnichsen, H. von Poschinger, G. von Plessen, T. A. Klar, and J. Feldmann, Appl. Phys. Lett. **81**, 171 (2002).
[14] K. C. Chu, C. Y. Chao, Y. F. Chen, Y. C. Wu, and C. C. Chen, Appl. Phys. Lett. **89**, 103107 (2006).
[15] P. R. Evans, G. A. Wurtz, W. R. Hendren, R. Atkinson, W. Dickson, A. V. Zayats, and R. J. Pollard, Appl. Phys. Lett. **91**, 043101 (2007).
[16] P. A. Kossyrev, A. Yin, S. G. Cloutier, D. A. Cardimona, D. Huang, P. M. Alsing, and J. M. Xu, Nano Lett. **5**, 1978 (2005).
[17] C. Huang, A. Bouhelier, G. Colas des Francs, G. Legay, J.-C. Weeber, and A. Dereux, Opt. Lett. **33**, 300 (2008).
[18] A. Bouhelier, M. Beversluis, A. Hartschuh, and L. Novotny, Phys. Rev. Lett. **90**, 013903 (2003).
[19] V. Fréedericksz and V. Zolina, Trans. Faraday Soc. **29**, 919 (1933).
[20] T. A. Milligan, *Modern Antenna Design* (Wiley, New York, 2005).
[21] C. Vena, C. Versace, G. Strangi, S. D'Elia, and R. Bartolino, Opt. Express **15**, 17063 (2007).